PROCEEDINGS OF SPIE

SPIEDigitalLibrary.org/conference-proceedings-of-spie

3D digital method and algorithm for the reconstruction of the polymer films polycrystalline structure

Zhengbing Hu, Olexander Ushenko, Artem Motrich, Alexander Dubolazov, Mykhailo Gavrylyak, et al.

Zhengbing Hu, Olexander Ushenko, Artem Motrich, Alexander Dubolazov, Mykhailo Gavrylyak, Iryna Soltys, Mykhailo Gorsky, Mykola Matymish, Olena Nanaka, Olena Kovalchuk, Patryk Panas, Magzhan Sarsembayev, "3D digital method and algorithm for the reconstruction of the polymer films polycrystalline structure," Proc. SPIE 12476, Photonics Applications in Astronomy, Communications, Industry, and High Energy Physics Experiments 2022, 124760H (12 December 2022); doi: 10.1117/12.2659297

SPIE.

Event: Photonics Applications in Astronomy, Communications, Industry, and High Energy Physics Experiments 2022, 2022, Lublin, Poland

3D digital method and algorithm for the reconstruction of the polymer films polycrystalline structure

Zhengbing Hu[a], Olexander Ushenko[b,c], Artem Motrich[b], Alexander Dubolazov[b], Mykhailo Gavrylyak[b], Iryna Soltys[b], Mykhailo Gorsky[b], Mykola Matymish[b], Olena Nanaka[d], Olena Kovalchuk[e], Patryk Panas[f], Magzhan Sarsembayev[g]
[a]School of Computer Science, Hubei University of Technology, Wuhan, China; [b]Chernivtsi National University, 2 Kotsiubynskyi Str., Chernivtsi, Ukraine; [c]Research Institute of Zhejiang University, Taizhou, China; [d]Vinnytsia National Technical University, Ukraine; [e]Vinnytsia National Medical University named M.Pirogov, Ukraine; [f]Lublin University of Technology, Lublin, Poland; [g]Al-Farabi Kazakh National University, Almaty, Kazakhstan

ABSTRACT

Proposed and substantiated a method for 3d mueller-matrix reproduction of the distributions of parameters of linear and circular birefringence and dichroism of partially depolarizing polymer films in publishing and printing business.

Keywords: 3D reconstruction, polymer film, Mueller matrix, depolarization.

1. INTRODUCTION

At present, methods and means of Mueller-matrix polarimetry (MMP) for the tasks of diagnostics of the structure of polymer films are being actively developed in biomedical optics. It includes a number of original directions: the study of scattering matrices and [1,2,3] and Mueller-matrix polarimetry [4,5,6] including computer assisted methods. The further development and generalization of the methods of MMP 3D polycrystalline structure of films with different multiplicity of light scattering, or different depolarizing ability is urgent [7,8,9].

Our work is aimed at developing a Mueller-matrix mapping method for reconstructing the distributions of the optical anisotropy parameters of partially depolarizing films of various polymers [10,11,12]

2. BRIEF THEORY OF THE METHOD

It is based on the use of a reference wave of laser radiation, which in the scheme of an optical interferometer is superimposed on a polarization-inhomogeneous image of a polymer film. The resulting interference pattern is recorded using a digital camera. Using diffraction integrals, the digital holographic reproduction of the distributions of the complex amplitudes $\{E_x(x,y);\quad E_y(x,y)\}$ of the object field of the polymer film is performed [13,14,15].

The technique of polarization-correlation determination of the distributions of the polarization ellipticity consists in the following set of actions [16,17,18]:

- Formation of planar polarization states in "irradiating" and "reference" laser beams.
- Registration of two partial interference patterns through the polarizer-analyzer 14 with the orientation of the transmission plane at angles $\Omega = 0°;\quad \Omega = 90°$.
- For each partial interference distribution, we perform a two-dimensional discrete Fourier transform $DFT(\upsilon,\nu)$ on the image. The two-dimensional $DFT(\upsilon,\nu)$ of a two-dimensional array $I_{\Omega=0°;90°}(x,y)$ (i.e. the image) is a function of two discrete variables coordinates (x,y) is defined by [10]:

Photonics Applications in Astronomy, Communications, Industry, and High Energy Physics Experiments 2022, edited by Ryszard S. Romaniuk, Andrzej Smolarz, Waldemar Wójcik, Proc. of SPIE Vol. 12476, 124760H
© 2022 SPIE · 0277-786X · doi: 10.1117/12.2659297

$$DFT_{\Omega=0°;90°}(\upsilon,\nu)=\frac{1}{M\times N}\sum_{x=0}^{M-1}\sum_{y=0}^{N-1}I_{\Omega=0°;90°}(x,y)\exp\left[-i2\pi\left(\frac{x\times\upsilon}{M}+\frac{y\times\nu}{N}\right)\right] \quad (1)$$

where $I_{\Omega=0°;90°}(x,y)=A_{\Omega=0°;90°}(x,y)A^{*}_{\Omega=0°;90°}(x,y)$ are the coordinate distributions of the intensity of the interference pattern filtered by the analyser with the orientation of its transmission axis at $\Omega=0°$; $\Omega=90°$; $A_{\Omega=0°;90°}(x,y)$ are the orthogonal projections of the complex amplitudes; * denotes the complex conjugation operation; (υ,ν) are the spatial frequencies in the x and y directions respectively; and (M,N) are the number of pixels of the CCD camera in the x and y directions respectively, such that $0\le x,\upsilon\le M$ and $0\le y,\nu\le N$.

- The results of this transformation should contain three peaks, one central (main) peak and two additional side peaks. DFT in the described case works like a low-pass filter. It removes carrier (interference fringes) which is used to extract complex representation of real field from object. Also, since the extracted part has limited size, it also acts like a low-pass filter for the object field too [19,20].
- Either of the additional side peaks (in complex representation) can be used to create a new Fourier spectrum by first extracting the peak and then placing it into centre of a newly generated spectrum $DFT_{\Omega=0°;90°}(\upsilon,\nu)$.
- Applying a two-dimensional inverse discrete Fourier transform $\left(DFT_{\Omega=0°;90°}\right)^{*}(x,y)$ on the obtained spectrum $DFT'_{0°;90°}(\upsilon,\nu)$, one gets:

$$\left(DFT_{\Omega=0°;90°}\right)^{*}(x,y)=\frac{1}{M\times N}\sum_{x=0}^{M-1}\sum_{y=0}^{N-1}DFT_{\Omega=0°;90°}(\upsilon,\nu)\exp\left[-i2\pi\left(\frac{x\times\upsilon}{M}+\frac{y\times\nu}{N}\right)\right]. \quad (2)$$

Here, $\left(DFT_{\Omega=0°;90°}\right)^{*}(x,y)\equiv A_{\Omega=0°;90°}(x,y)$.

- One subsequently obtains (for each state of polarization $\{Ir-\mathrm{Re}\}$) a distribution of complex amplitudes [21] in different phase planes:

$$\begin{cases}\Omega_{0°}\to|A_0|;\\ \Omega_{90°}\to|A_{90}|\exp\left(i\left(\delta_{90°}-\delta_{0°}\right)\right)\end{cases} \quad (3)$$

The phase planes are defined by:

$$\theta_k=\left(\delta_{90°}-\delta_{0°}\right)=\frac{2\pi}{\lambda}\Delta nz;\ \ 0\le z\le h \quad (4)$$

where Δn is the birefringence; λ is the wavelength; and h is the sample thickness of the object field, separated by an arbitrary step of $\Delta\theta$.

- In each phase plane θ_k the corresponding sets of and polarization parameters (elipticity β) of the object field of the biological layer are calculated [22]:

$$\begin{aligned}S_1(0°,90°,45°,\otimes)&=|E_x|^2+|E_y|^2;\\ S_2(0°,90°,45°,\otimes)&=|E_x|^2-|E_y|^2;\\ S_3(0°,90°,45°,\otimes)&=2\,\mathrm{Re}|E_xE_y^{*}|;\\ S_4(0°,90°,45°,\otimes)&=2\,\mathrm{Im}|E_xE_y^{*}|.\end{aligned} \quad (5)$$

Here $0°,90°,45°$ - polarization azimuths of linearly polarized irradiating beams, $\otimes$ - right circularly polarized beam.

Further, based on relations (1), the set of elements of the Mueller matrix is calculated using the following Stokes-polarimetric relations:

$$\{M\} = 0,5 \begin{Vmatrix} \left(S_1^0 + S_1^{90}\right) & \left(S_1^0 - S_1^{90}\right) & \left(S_1^{45} - S_1^{135}\right) & \left(S_1^{\otimes} - S_1^{\oplus}\right) \\ \left(S_2^0 + S_2^{90}\right) & \left(S_2^0 - S_2^{90}\right) & \left(S_2^{45} - S_2^{135}\right) & \left(S_2^{\otimes} - S_2^{\oplus}\right) \\ \left(S_3^0 + S_3^{90}\right) & \left(S_3^0 - S_3^{90}\right) & \left(S_3^{45} - S_3^{135}\right) & \left(S_3^{\otimes} - S_3^{\oplus}\right) \\ \left(S_4^0 + S_4^{90}\right) & \left(S_4^0 - S_4^{90}\right) & \left(S_4^{45} - S_4^{135}\right) & \left(S_4^{\otimes} - S_4^{\oplus}\right) \end{Vmatrix}. \quad (6)$$

Traditionally, on the right side of expressions (2), the value of the phase shift $\delta(z = l)$ integral over the entire thickness l of the biological layer "appears". Therefore, the results of direct Mueller-matrix mapping are two-dimensional distributions of the values of matrix elements $M_{ik} = q_j\left(S_{z=1;2;3;4}(x, y, \delta)\right)$ averaged ($\delta(z = l)$) over the entire thickness l of the polymer film. In the case of using a coherent reference wave and digital holographic reproduction algorithms, it becomes possible to reproduce the distributions of the complex amplitudes $|E_x|\exp i(\Delta\delta_x)$; $|E_y|\exp i(\Delta\delta_y)$ of the object field in a discrete $(\Delta\delta_{l=0....q})$ set of phase planes $\boldsymbol{\delta}$. Due to this, it is possible to obtain a set of layer-by-layer distributions of the magnitude of matrix elements ($x, y, k\Delta\delta$) and determine their volumetric structure

$$M_{ik} = \left\{g_s\left(|E_x|, |E_y|, \delta^*\right)\right\}\left(x, y, \begin{pmatrix} 0 \\ \Delta\delta \\ . \\ \delta \end{pmatrix}\right). \quad (7)$$

3. OPTICAL SCHEME AND 3D MUELLER-MATRIX POLARIMETRY TECHNIQUE

Figure 1 shows the configuration of the optical system of 3D Mueller-matrix polarimetry of a polymer film. Parallel beam of He-Ne laser 1, formed by spatial-frequency filter 2, with 50/50 beam splitter 5 is divided into "object" and "reference" ones. The input polarization state formed by quarter wave plate 3 and polarizer 4 is linear with azimuth 00 (perpendicular) with respect to the XY plane. The "object" beam with the help of a rotating mirror 8 is directed through the polarizing filter 9 - 11 in the direction of the sample of the biological layer 15. The polarization-inhomogeneous image of the object 15 is projected by the strain-free objective 17 into the plane of the digital camera 18. The "reference" beam is directed by the mirror 7 through the polarization filter 12 - 14 into the plane of the polarization-inhomogeneous image of the object 15. As a result, an interference pattern is formed, the coordinate intensity distribution of which is recorded by a digital camera 18.

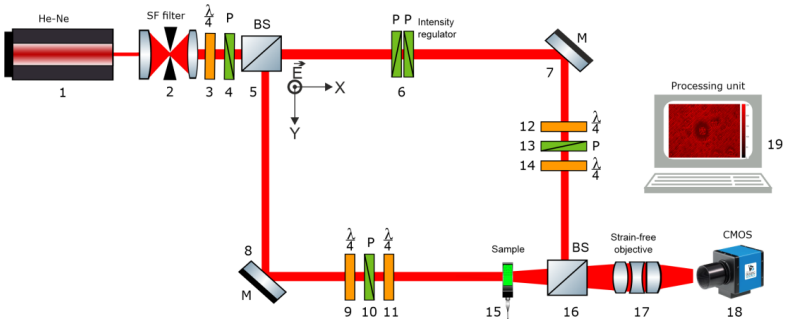

Figure 1. Diagram of polarization interferometry of 3D distributions of the elements of the Mueller matrix. Explanations in the text.

The technique of polarization-interference determination of the elements of the Mueller matrix consists in the following set of actions:

- Formation of six polarization states in the irradiating and reference laser beams - $(0°-0°)$; $(90°-90°)$; $(45°-45°)$; $(135°-135°)$; $(\otimes-\otimes)$; $(\oplus-\oplus)$.
- Registration of each partial interference pattern through the polarizer-analyzer 14 with sequential orientation of the transmission plane at angles $\Omega = 0°$; $\Omega = 90°$.

4. METHODS FOR OBJECTIVE ASSESSMENT OF POLARIZATION MAPS

For an objective assessment of layer-by-layer polarization maps $S(\theta_k, x, y)$, the statistical moments of the first (Z_1), second (Z_2), third (Z_3) and fourth (Z_4) orders were used, which were calculated by the following algorithms [8]

$$\begin{aligned} Z_1 &= \frac{1}{N}\sum_{j=1}^{N} S(\theta_k, x, y)_j; \\ Z_2 &= \sqrt{\frac{1}{N}\sum_{j=1}^{N}\left(S^2(\theta_k, x, y)\right)_j}; \\ Z_3 &= \frac{1}{Z_2^3}\frac{1}{N}\sum_{j=1}^{N}\left(S^3(\theta_k, x, y)\right)_j; \\ Z_4 &= \frac{1}{Z_2^4}\frac{1}{N}\sum_{j=1}^{N}\left(S^4(\theta_k, x, y)\right)_j, \end{aligned} \tag{8}$$

where N – number of pixels of the photosensitive area of the CCD camera.

The statistical moment of the 1st order determines the average value of the coordinate distribution of the optical anisotropy parameters. The statistical moment of the 2nd order characterizes the spread of random values of linear birefringence and dichroism. The third-order statistical moment characterizes the asymmetry of the distribution of optical anisotropy parameters. The fourth-order statistical moment characterizes the sharpness of the peak in the distribution of structural anisotropy parameters. To determine the optimal phase plane, we used a two-stage algorithm for analyzing layer-by-layer maps of the optical anisotropy. At the first stage:

- Selected step of discrete phase "macro" scanning $\Delta\theta_k^{\max} = 0.25\text{rad}$.
- Algorithmically reconstructed a series of corresponding to each $\Delta\theta_k^{\max} = 0.25\text{rad}$ layer-by-layer coordinate distributions of the magnitude of the $S(x, y, \theta_k)$.
- Statistical moments of the 1st - 4th orders $Z_{i=1;2;3;4}$, which characterize the obtained 2D distributions $S(x, y, \theta_k)$, were calculated.
- The difference between the values of each of the statistical moments of the 1st - 4th orders was calculated $(\Delta Z_i)_k = Z_i(\theta_{j+1}^{\max}) - Z_i(\theta_j^{\max})$.
- The phase interval $\Delta\theta^* = (\theta_{j+1}^{\max} \div \theta_j^{\max})$ was determined, within which the monotonic growth of the value $\Delta Z_i = Z_i(\theta_{j+1}^{\max}) - Z_i(\theta_j^{\max}) \le 0$ stops.
- Within the limits $\Delta\theta^*$, a new series $\Delta Z_i = Z_i(\theta_{q+1}^{\min}) - Z_i(\theta_q^{\min})$ of values was calculated with a discrete phase "micro" scan step $\Delta\theta_q^{\min} = 0.05\text{rad}$.
- The optimal phase plane θ^* was determined, in which $\Delta Z_i(\theta^*) = \max$.

The proposed technique provides the possibility of algorithmic recovery of the values of linear birefringence and dichroism by measuring the set of elements of the Mueller matrix and analytically calculating the parameters of the first-order differential matrix. This matrix characterizes the average values of the parameters of the phase (linear and circular birefringence) and amplitude (linear and circular dichroism) anisotropy of the phase-inhomogeneous polymer layer. Calculations of the distributions of optical anisotropy parameters are presented (Fig. 2).

Analysis of the obtained maps of optical anisotropy showed:

1. The presence of a wide range of variation in the values of the parameters of linear birefringence and dichroism of polymer layers.
2. Coordinate heterogeneity of reconstructed maps of structural phase and amplitude anisotropy.
3. Individual and statistically distributed topographic domain structure of optical anisotropy polymer layers polarization maps.

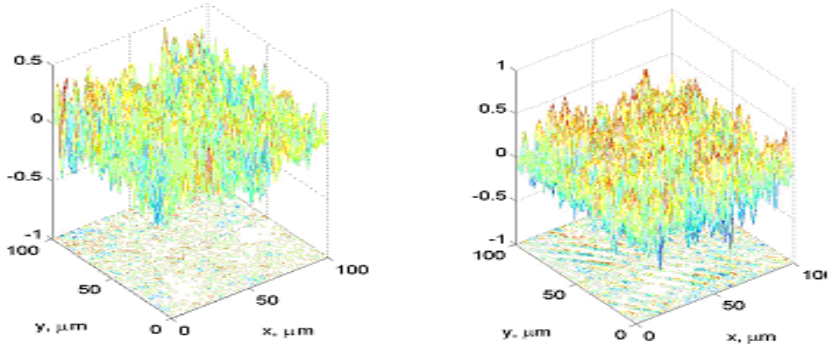

a) b)

Figure 2. 3D maps of distributions of linear birefringence (a) and dichroism (b) of a partially depolarizing polycrystalline film.

The morphological structure of phase-inhomogeneous polymer layers is characterized by:

1. The presence of a distant order - spatially ordered fibers that form the so-called structural anisotropy or linear birefringence
2. The presence of close order - cluster domains of optically active molecules, which form the so-called circular birefringence.

The way out of this situation is the method of layer-by-layer polarization-holographic 3D scanning.

5. CONCLUSIONS

A method for 3D Muller-matrix reproduction of the distributions of the parameters of linear and circular birefringence and dichroism of partially depolarizing polycrystalline films is proposed and substantiated.

The dynamics of the change in the value of the statistical moments of the 1st - 4th orders, characterizing the distributions of the optical anisotropy parameters of a polycrystalline polymer film in various "phase" sections of its volume, has been investigated and analyzed.

ACKNOWLEDGEMENTS

This work received funding from National Research Foundation of Ukraine, Project 2020.02/0061 and Grant SDGF/VDE4/670/2022-421 by OUN.

REFERENCES

[1] Mishchenko, M. I., Travis, L. D., and Lacis, A. A., [Scattering, Absorption, and Emission of Light by Small Particles], Cambridge University Press, Cambridge (2002).
[2] Swami, M. K., Patel, H. S., and Gupta, P. K., "Conversion of 3 × 3 Mueller matrix to 4 × 4 Mueller matrix for non-depolarizing samples, " Opt. Commun. 286(1), 18–22 (2013).

[3] Izotova, V. F., et al., "Investigation of Mueller matrices of anisotropic nonhomogeneous layers in application to optical model of cornea, " Appl. Opt. 36(1), 164–169 (1997).
[4] Tuchin, V. V., "Tissue optics and photonics: biological tissue structures [review]," J. Biomed. Photonics Eng. 1(1), 3–21 (2015).
[5] Tuchin, V. V., "Tissue optics and photonics: light-tissue interaction [review]," J. Biomed. Photonics Eng. 1(2), 98–134 (2015).
[6] Hu, Z., Ivashchenko, M., Lyushenko, L., Klyushnyk, D., "Artificial Neural Network Training Criterion Formulation Using Error Continuous Domain," International Journal of Modern Education and Computer Science 13(3), 13-22 (2021).
[7] Hu, Z., Tereikovskyi, I., Chernyshev, D., Tereikovska, L., Tereikovskyi, O., Wang, D., "Procedure for Processing Biometric Parameters Based on Wavelet Transformations," International Journal of Modern Education and Computer Science 13(2), 11-22 (2021).
[8] Manhas, S., Swami, M. K., Buddhiwant, P., Ghosh, N., Gupta, P. K., Singh, K., "Mueller matrix approach for determination of optical rotation in chiral turbid media in backscattering geometry," Opt. Express 14(1), 190–202 (2006).
[9] Deng, Y., Zeng, S., Lu, Q., Luo Q., "Characterization of backscattering Mueller matrix patterns of highly scattering media with triple scattering assumption," Opt. Express 15(15), 9672–9680 (2007).
[10] Wang, X., and Wang, L. V., "Propagation of polarized light in birefringent turbid media: a Monte Carlo study, " J. Biomed. Opt. 7(3), 279–290 (2002).
[11] Hadley, K.C., Vitkin, I.A. "Optical rotation and linear and circular depolarization rates in diffusively scattered light from chiral, racemic, and achiral turbid media," J. Biomed. Opt. 7(3), 291–299 (2002).
[12] Tuchin, V.V., Wang,, L., Zimnyakov, D.A., [Optical Polarization in Biomedical Applications], Springer, New York (2006).
[13] De Martino, Ed., "A polarization-based optical techniques applied to biology and medicine," in Proc. European Workshop, Ecole Polytechnique, Massy, France (2009).
[14] Dubolazov, A., Ushenko, V., Trifonyuk, L., Stashkevich, A., Soltys, I., Ushenko, Y., Tomka, Y., Ushenko, A., Gantyuk, V., Gorodensky, P., "Polarization-Singular Approach to Imaging Mueller-Matrix Polarimetry in the Differential Diagnosis of Histological Sections of Biopsy of Tumors of the Uterus and Prostate," Frontiers in Physics, 9, 711212 (2021).
[15] Litvinenko, A., Tryfonyuk, L., Pavlyukovich, O., Pavlyukovich, N., Stashkevich, A.T., Olar, O., Kurek, O.I., Tkachuk, V.I., "Polarization mapping of laser-induced monospectral fields of optically anisotropic fluorophores in forensic diagnostics of the age of the formation of damage to human organsb" Proc. SPIE 12126, 1212622 (2021).
[16] Stashkevich, A.T., Wanchulyak, O.Y., Litvinenko, O.Y., Ushenko, Y.O., Dubolazov, O.V., Sorochan, E., Zagoruiko, L.V., Wójcik, W., Rakhmetullina, S., Denissova, N., Jarykbassov, D., "Differential Mueller-matrix tomography of the polycrystalline structure of biological tissues with different damage durations," Proc. 12040, 120400G (2021).
[17] Stashkevich, A.T., Kozan, N.R., Oliynik, I.Y., Hulei, L.V., Polevoy, V.P., Solovey, Y.M., Ushenko, Y.O., Dubolazov, O.V., Paliy, V.G., Wójcik, W., Duskazaev, G., Zhunissova, U., Jarykbassov, D., Multiparameter polarization-phase microscopy of optically anisotropic networks of biological crystals," Proc. SPIE 12040, 120400F (2021).
[18] Stashkevich, A.T., Dunaiev, O.V., Kvasniuk, D.V., Polevoy, V.P., Solovey, Y.M., Chepega, I.G., Ushenko, Y.O., Dubolazov, O.V., Paliy, V.G., Kisała, P., Ormanbekova, A., Tungatarova, A., "Spectral polarimetry of laser images of biological fluid layers in the differentiation of necrotic conditions" Proc. SPIE 12040, 120400C (2021).
[19] Rovira, J. R., Pavlov, S. V., Vassilenko, V. B., Wójcik, W. and Sugurova, L., "Methods and resources for imaging polarimetry, " Proc. SPIE, 86980T (2013).
[20] Wójcik, W., Pavlov, S., Kalimoldayev, M., [Information Technology in Medical Diagnostics II], Taylor & Francis Group CRC Press, London (2019).
[21] Ushenko, A. G., and Olar, O., “Differential diagnostics of aseptic and septic loosening of the cup of the endoprosthesis of the artificial hip joint by the methods of polarisation tomography,” IAPGOS 9(3), 22-25 (2019).
[22] Zabolotna, N.I, Okarskyi, H.H., Pavlov, S.V., "ROC analysis of informativeness of mapping of the ellipticity distributions of blood plasma films laser images polarization in the evaluation of pathological changes in the breast," Proc. SPIE 11456, 114560I (2020).